Chin. J. Astron. Astrophys. Vol. 7 (2007), No. 4, 531–538
(*http://www.chjaa.org*)

Chinese Journal of
Astronomy and
Astrophysics

Measuring the Distance of VX Sagittarii with SiO Maser Proper Motions *

Xi Chen[1,2], Zhi-Qiang Shen[1] and Ye Xu[1]

[1] Shanghai Astronomical Observatory, Chinese Academy of Sciences, Shanghai 200030; *chenxi@shao.ac.cn*
[2] Department of Earth Sciences, National Taiwan Normal University, 88 Sec. 4, Ting-Chou Rd., Taipei 116, Taiwan

Received 2006 December 12; accepted 2007 April 27

Abstract We report on 43 GHz v=1, J=1–0 SiO maser proper motions in the circumstellar envelope of the M-type semi-regular variable star VX Sgr, observed by Very Long Baseline Array (VLBA) at 3 epochs during 1999 April–May. Applying the statistical parallax analysis to these proper motions, we estimated a distance of VX Sgr of 1.57$\pm$0.27 kpc, which is consistent with that based on the proper motions of H_2O masers, or on the assumption that VX Sgr belongs to the Sgr OB1 association. At this distance, VX Sgr can be classified as a red supergiant. Comparing the statistical parallax method with those of model fitting and annual parallax, we think that the statistical parallax method may be a good way of estimating SiO maser distances at present.

Key words: methods: statistical — masers — stars: individual (VX Sgr) — stars: distances

1 INTRODUCTION

VX Sagittarii (VX Sgr) is a semi-regular variable with a long, mean optical pulsation period of 732 days (Kukarkin et al. 1970). Its spectral type ranges from M4e Ia to M9.8, and the stellar temperature is between 2400 and 3300 K (Lockwood & Wing 1982). Its circumstellar envelope exhibits strong OH, H_2O and SiO maser radiation (Chapman & Cohen 1986; Greenhill et al. 1995; Marvel et al. 1998; Murakawa et al. 2003; Kamohara et al. 2005). The systemic velocity of VX Sgr is estimated to be about 5.3 km s^{-1} based on a dynamical model of an expanding envelope fitted to the interferometric maps of OH maser emission at 1612 MHz (Chapman & Cohen 1986).

VX Sgr is classified as a red supergiant. This classification, however, strongly depends on its distance measurement, which is a topic of some debate. The distance to VX Sgr is uncertain by a factor of $>$6 ranging between 0.3 to 2.0 kpc (see Table 1). VX Sgr would probably not be classified as a supergiant if it were at the nearest distance, and then it would not be one of the most luminous stars known. Therefore, it is crucial to measure the distance as accurately as possible.

In Table 1, we list all the published measurements of the distance to VX Sgr in the literature. These should be taken with caution because of the following facts. There is no compelling reasons to believe that VX Sgr is associated with the Sgr OB1 association. The photometric distance could be underestimated due to the larger uncertainty in determining the interstellar extinction for VX Sgr and its strong variation in luminosity. The typical 1 mas precision of Hipparcos parallax makes it hard to determine a distance greater than 0.1 kpc with 10% uncertainty. At a galactic longitude of 8°, VX Sgr did not have a meaningful kinematic distance (known to be ambiguous with values of 4.5 and 15.5 kpc, Humphreys 1974) until the

* Supported by the National Natural Science Foundation of China.

Table 1 Existing Distance Estimate of VX Sgr

Distance (kpc)	Method	Ref.
1.7–2.0	OB association	1, 2, 3
0.8	photometry	4
0.238	photometry	5
0.41	assuming an $L_{\rm bol}$=$10^5 L_\odot$ for M supergiant	6
1.7±0.3	proper motions of H_2O masers (VLBA)	7
1.8±0.5	proper motions of H_2O masers (MERLIN)	8
0.3–0.5	trigonometric parallax (Hipparcos, HIP 88838)	9

[1] Morgan, Whitford & Code (1953); [2] Alter, Balázs & Ruprecht (1970); [3] Humphreys, Strecker & Ney (1972); [4] Humphreys (1974); [5] Celis (1975); [6] Loup et al. (1993); [7] Marvel, Diamond & Kemball (1998); [8] Murakawa et al. (2003); [9] Pourbaix et al. (2003), the Hipparcos Catalogue number of VX Sgr is HIP 88838.

proper motions were obtained of its H_2O masers. This is based on the assumption that the observed proper motions and Doppler velocities fully sample the circumstellar shell, which may or may not be the case.

Astronomical masers are a good tool for measuring distances in our Milky Way. The distance to VX Sgr obtained from the proper motions of H_2O masers was about 1.7–1.8 kpc, consistent with the generally adopted value of 1.7 kpc (Murakawa et al. 2003). In this paper, we report a distance measurement with SiO maser proper motions in VX Sgr.

2 OBSERVATIONS AND DATA REDUCTIONS

The 43 GHz v=1, J=1–0 SiO maser emission toward VX Sgr was observed at 3 epochs (in 39 days), 1999 April 24, May 23 and May 31, using the Very Long Baseline Array (VLBA) of the NRAO [1]. The adopted position of VX Sgr in our observations was $18^{\rm h}08^{\rm m}04^{\rm s}.062$ (R.A.) and $-22^\circ13'26''.10$ (J2000) (Dec.). The data were recorded in left circular polarization in an 8 MHz band and correlated with the FX correlator in Socorro, New Mexico. The correlator output data had 256 spectral channels, corresponding to a velocity spacing of 0.22 km s^{-1}. The data reduction followed standard procedures using the Astronomical Image Processing System (AIPS) package, the details of which have been described previously by Chen et al. (2006, Paper I hereafter).

The definition of "maser spot" and "maser feature" and the identification of the maser features have been described in Paper I. A maser spot is a single velocity component of the maser emission, reflecting somewhat instrumental factors, especially the velocity spacing of each channel. A maser feature is a group of maser spots within a small region in space and Doppler velocity, typically 1 AU and 1 km s^{-1}, and is expected to be a physical feature consisting of a single gas clump. In order to study the characteristics of SiO masers, individual features were determined for each of the three epochs, and 110, 110 and 105 maser features were finally identified for epoch 1, 2 and 3, respectively.

3 RESULTS

3.1 Proper Motions

The typical lifetime of an SiO maser feature that is both spatially and velocity coherent, is of order one month. This limits the time interval of the monitoring observations to measure their proper motions. Our 3-epoch observations spanning 39 days show that some SiO maser features lived through the three epochs (see fig. 3 of Paper I). This enabled us to study their proper motions and hence the kinematics of the circumstellar envelope of VX Sgr by comparing the features that appeared in all the three epochs.

We have confirmed 42 matched features in all three observing sessions (Paper I). Because of the nature of standard VLBI data reduction, the absolute position of the phase center in each image is lost. For studying the individual proper motions, we must line up multi-epoch maps. The feature used for registration is the one with a velocity $V_{\rm LSR}$ ≈0 km s^{-1} at all the three epochs. This feature was chosen because of its similarity in both morphology and velocity. The coordinate frames for the three epochs were then shifted so as to put this feature at the origin (0, 0). The process of aligning the maps of the three epochs on a feature located on

[1] The National Radio Astronomy Observatory is a facility of the National Science Foundation operated under cooperative agreement by Associated Universities, Inc.

the shell could introduce a systematic bias in the proper motion estimates; individual maser proper motions are uncertain by a constant offset vector that represents the motion of the reference feature. We assumed that the average of the proper motions for all the matched features represents the motion of the alignment feature. In order to present a better representation of the actual motions of individual features, the mean proper motion was subtracted from all the determined proper motion vectors.

Table 2 lists the proper motions of matched features between epochs 1 and 2, and between epochs 1 and 3. The uncertainty in the R.A. motion for each matched feature was estimated by $\sigma_{\mu_x} = \sqrt{\sigma_{x1}^2 + \sigma_{x2}^2}/\Delta t$, where σ_{x1} and σ_{x2} are the position errors of matched feature in R.A. at the two epochs, and Δt is the time separation between two epochs. The uncertainty in the Dec. motion is estimated in the same way.

Table 2 Proper Motions of SiO Maser Features in VX Sgr

Position Epoch 1			Proper motions Epoch 1-Epoch 2				Epoch 1-Epoch 3			
V_{LSR} (km s^{-1})	x (mas)	y (mas)	μ_x (mas yr^{-1})	σ_{μ_x}	μ_y (mas yr^{-1})	σ_{μ_y}	μ_x (mas yr^{-1})	σ_{μ_x}	μ_y (mas yr^{-1})	σ_{μ_y}
(1)	(2)	(3)	(4)	(5)	(6)	(7)	(8)	(9)	(10)	(11)
12.61	–1.010	–14.191	0.005	0.143	1.062	0.566	–0.077	0.112	1.055	0.346
11.41	–2.476	1.010	0.511	0.453	1.088	0.889	–0.086	0.408	1.205	0.759
10.91	–17.394	–13.077	1.370	0.156	–0.915	0.521	1.427	0.102	–1.916	0.362
9.56	–2.447	2.603	–0.372	0.577	–1.642	1.097	–0.405	0.492	–1.251	0.860
9.00	–0.816	3.522	–0.160	0.053	–0.217	0.421	–0.213	0.045	–0.363	0.355
8.02	–19.006	–11.645	0.776	0.271	0.415	0.795	0.786	0.211	0.316	0.617
7.93	–19.192	–10.487	1.514	0.554	2.034	1.042	1.365	0.440	1.434	0.833
7.86	–1.874	3.840	–0.811	0.480	–0.174	0.332	–0.803	0.394	–0.500	0.377
7.17	–0.591	2.829	–0.585	0.173	–0.081	0.394	–1.044	0.320	–1.469	0.815
6.84	–19.553	–11.422	0.894	0.273	–0.973	0.627	1.217	0.254	–0.080	0.670
6.60	–6.365	5.655	–0.838	0.149	0.443	0.099	–0.715	0.129	0.063	0.091
6.28	–21.632	–7.501	1.011	0.081	0.405	0.355	1.135	0.066	0.282	0.271
6.19	0.431	5.829	-0.029	0.128	0.743	0.536	–0.100	0.111	0.407	0.406
6.11	–1.270	5.285	–0.135	0.191	0.475	0.529	0.143	0.162	0.656	0.408
5.45	–6.999	5.063	0.323	0.178	–0.318	0.191	0.257	0.140	–0.418	0.156
5.37	–0.410	5.122	–0.054	0.548	0.977	0.565	0.024	0.350	0.307	0.412
5.32	3.134	0.891	0.891	0.208	0.474	0.574	0.598	0.239	0.140	0.421
4.94	–0.547	3.340	–1.176	0.272	0.001	0.585	–1.037	0.119	0.065	0.376
4.92	1.797	–0.044	–1.502	0.341	1.161	0.494	0.031	0.121	–0.881	0.575
4.67	3.964	0.075	0.728	0.471	–0.156	0.403	–1.349	0.547	–0.937	0.717
4.45	6.025	–1.322	0.138	0.352	–0.131	0.930	–0.303	0.250	–0.135	0.716
3.50	2.026	0.476	1.524	0.449	–0.800	0.688	1.277	0.407	0.527	0.431
3.31	5.400	–3.989	–1.390	0.392	0.045	0.937	–1.115	0.298	–0.362	0.708
3.28	0.406	5.000	–0.253	0.160	1.012	0.452	–0.178	0.129	0.534	0.396
3.17	–11.558	1.507	0.088	0.362	–1.675	0.646	-0.119	0.264	–0.781	0.525
2.54	4.862	–2.501	–1.204	0.129	–0.075	0.265	–0.561	0.444	0.276	0.715
2.45	4.317	–9.857	1.283	0.465	1.024	0.396	0.561	0.338	0.805	0.319
2.31	–9.234	5.303	–0.938	0.245	–0.911	0.529	–0.847	0.238	–0.633	0.833
2.06	–3.417	–0.244	0.425	0.257	0.598	0.182	0.310	0.204	0.613	0.155
1.46	–8.600	6.395	–0.446	0.163	–1.002	0.277	–0.259	0.133	–0.646	0.217
1.38	4.738	–9.977	0.162	0.278	–0.056	0.385	0.412	0.478	0.520	0.386
1.12	6.113	–9.991	–1.403	0.698	–1.066	0.532	0.775	0.482	–0.468	0.397
0.90	3.959	–5.067	–0.316	0.301	–0.552	0.473	–0.944	0.238	0.774	0.213
0.74	4.981	–9.771	0.283	0.131	0.175	0.136	0.455	0.144	–0.011	0.128
0.07 ^{r}	0.000	0.000	0.048	0.074	–0.094	0.228	0.082	0.068	–0.111	0.182
–0.33	4.275	–3.324	–0.099	0.190	–1.725	0.580	–0.250	0.215	–0.584	0.345
–0.90	5.114	–9.818	–0.085	0.072	–0.120	0.210	–0.309	0.182	–0.122	0.140
–1.22	–8.239	1.805	–0.541	0.193	–0.242	0.314	–0.576	0.130	0.222	0.331
–1.94	1.945	–18.794	0.023	0.091	0.457	0.205	–0.001	0.079	0.656	0.177
–2.00	6.491	–8.510	0.379	0.156	–0.123	0.204	0.371	0.108	–0.180	0.154
–3.71	2.612	–4.860	0.410	0.307	0.049	0.297	–0.036	0.245	0.097	0.229
–6.17	–14.401	5.235	0.017	0.106	0.412	0.428	0.102	0.094	0.895	0.291

Note.— columns (1)–(3): matched feature velocity and positions in R.A. and Dec. at epoch 1; columns (4)–(7): individual proper motion and its uncertainty in R.A. and Dec. between epoch 1 and epoch 2; columns (8)–(11): individual proper motion and its uncertainty in R.A. and Dec. between epoch 1 and epoch 3. r, the reference feature used to align three epoch maps.

The proper motions from epoch 1 to epoch 3 are shown in Figure 1. These proper-motion vectors are relatively random, and do not convey any distinct visual impression of expansion or contraction, although a dominant inward velocity of about 4 km s^{-1} of the SiO maser shell was obtained from their pairwise separations for an assumed distance of 1.7 kpc to VX Sgr (Paper I).

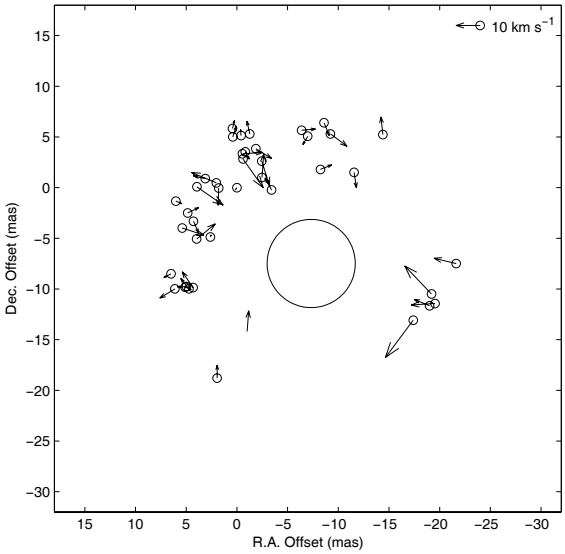

Fig. 1 Distribution of proper motion velocity vectors from epoch 1 to epoch 3 for an assumed distance of 1.7 kpc. The length of the vector is proportional to the velocity of the feature. The mean proper motion vector has been subtracted from each of the determined proper motion vectors.

3.2 Distance to VX Sgr

The proper motions of the masers can be used to derive the distance to the source from a statistical relation of transverse and radial velocities. If the spatial motions of the maser features are random, then the dispersion of the angular motion in R.A. and Dec. (proper motion), σ_μ, can be compared with the dispersion of the spatial motion along the line of sight (radial velocity) σ_v, and so giving an estimate of the distance D, according to the formula,

$$D = \sigma_v / \sigma_\mu. \tag{1}$$

This is the "statistic parallax" method, which has been applied to measure distances to water maser sources e.g., W51 Main (Genzel et al. 1981a) and W51 North (Schneps et al. 1981). We can now apply this method to measure the distance of the SiO masers around VX Sgr.

The top panel of Figure 2 shows the distribution of radial velocities for all the detected 325 features at the three epochs. The middle and bottom panels similarly refer to the transverse motions from epoch 1 to epoch 2 and from epoch 1 to epoch 3. The systemic velocity along the line of slight of VX Sgr of 5.3 km s^{-1} (Chapman & Cohen 1986) was used to calculate the radial velocity dispersion σ_v. The radial velocity dispersion with respect to the systemic velocity of VX Sgr is 4.81 km s^{-1} for all the detected features at the three epochs. The dispersions of the transverse motions were calculated with respect to the mean proper motions in R.A. and Dec. The average of the proper motions for all matched features representing the motion of the alignment feature was subtracted from these proper motions (see Section 3.1), thus the mean values of threse proper motions are zero in R.A. and Dec. The observed dispersions, $\sigma_\mu^{\rm obs}$, in R.A. and Dec. with respect to the mean are 0.78 and 0.82 mas yr^{-1} for epoch 2-epoch 1, and 0.70 and 0.72 mas yr^{-1} for epoch 3-epoch 1, respectively. These dispersion values in R.A. and Dec. are also indicated by the horizontal arrows in the middle and bottom panels of Figure 2.

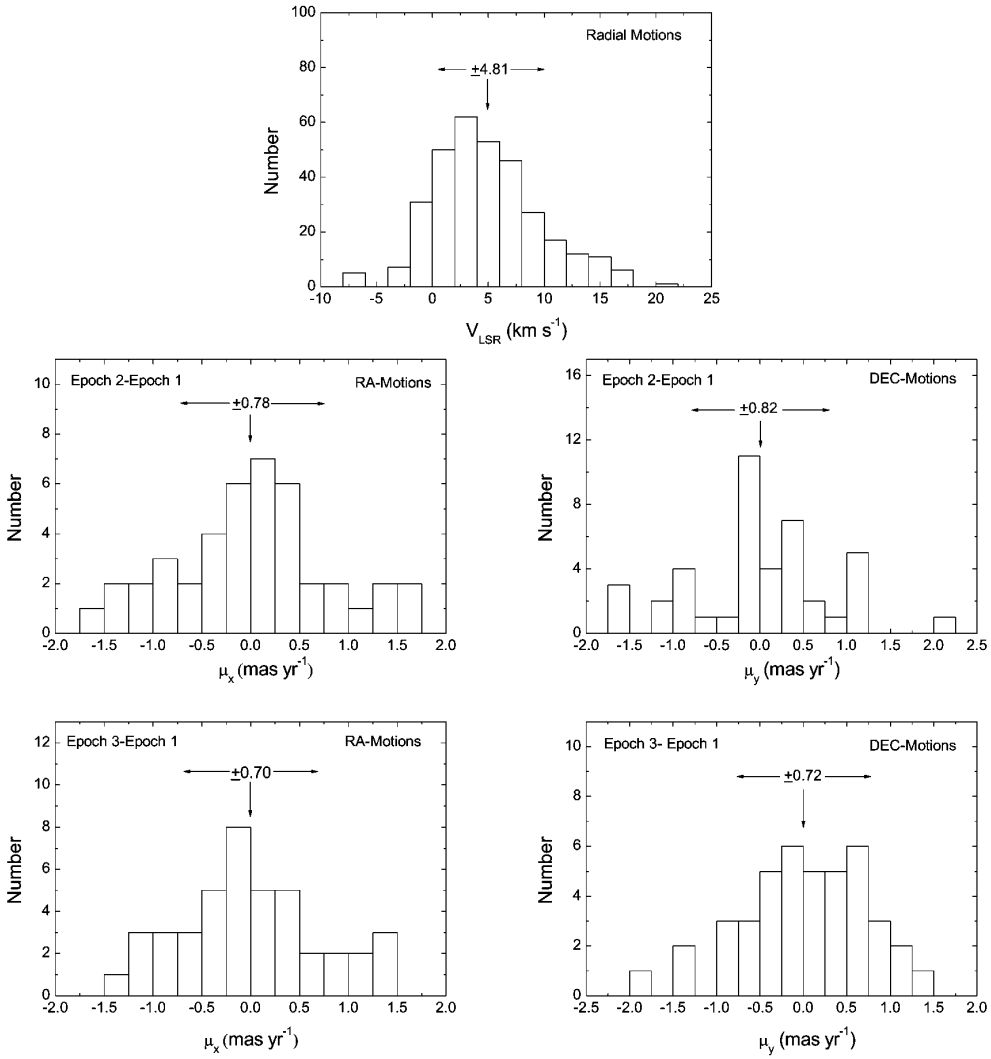

Fig. 2 Top panel: Histogram of radial velocities (relative to the LSR) for all the detected 325 features at the three epochs. The radial velocity dispersion (as indicated by the horizontal arrow) with respect to the systemic velocity of 5.3 km s^{-1} (indicated by the vertical arrow) of VX Sgr is 4.81 km s^{-1}. Middle and bottom panels show histograms of proper motions in R.A. and Dec. from epoch 1 to epoch 2 and from epoch 1 to epoch 3, respectively. The observational dispersions of proper motions in R.A. and Dec. (horizontal arrows) all refer to the mean values of these proper motions (vertical arrows).

To obtain the actual proper motion dispersion σ_μ, we need to correct the dispersions of proper motions for broadening by their measurement uncertainties $\epsilon_{\rm obs}$ (i.e. σ_{μ_x} in R.A., and σ_{μ_y} in Dec.; see columns 5 and 9, and columns 7 and 11 of Table 2). The actual proper motion can be written with the formula

$$\sigma_\mu^2 = (\sigma_\mu^{\rm obs})^2 - \langle\epsilon_{\rm obs}^2\rangle \pm 2\langle\mu\cdot\epsilon_{\rm obs}\rangle, \quad (2)$$

where the symbol $\langle\ \rangle$ denotes the mean. In our observations, the statistical errors $\langle\epsilon_{\rm obs}^{\,2}\rangle^{1/2}$ due to measurement noise are 0.31 mas yr^{-1} and 0.54 mas yr^{-1} in R.A. and Dec. between epoch 1 and epoch 2, and 0.27 mas yr^{-1} and 0.48 mas yr^{-1} in R.A. and Dec. between epoch 1 and epoch 3, respectively. Because the

Table 3 The Estimated Parameters of Calculating Distances

		σ_v (km s^{-1})	$\sigma_\mu^{\rm obs}$ (mas yr^{-1})	$\langle\epsilon_{\rm obs}^2\rangle^{1/2}$ (mas yr^{-1})	σ_μ (mas yr^{-1})	D (kpc)	σ_D (kpc)
Epoch 2–1	R.A.	4.81	0.78	0.31	0.72	1.40	0.17
	Dec.	4.81	0.82	0.54	0.62	1.63	0.24
Epoch 3–1	R.A.	4.81	0.70	0.27	0.65	1.55	0.19
	Dec.	4.81	0.72	0.48	0.54	1.87	0.28

value of $\langle\mu\cdot\epsilon_{\rm obs}\rangle$ is far smaller than that of $\langle\epsilon_{\rm obs}^2\rangle$, we ignore the term of $\langle\mu\cdot\epsilon_{\rm obs}\rangle$ in our calculations. Finally, we obtain the actual proper motion dispersions, σ_μ, in R.A. and Dec., to be 0.72 and 0.62 mas yr^{-1} between epoch 1 and epoch 2, and 0.65 and 0.54 mas yr^{-1} between epoch 1 and epoch 3. In general, the radial velocity dispersion is also broadened by its measurement uncertainty. The measurement uncertainty of radial velocity dispersion of about 0.35 km s^{-1}, obtained from the square root of the squared sum of (1) the standard deviation in the radial velocity dispersion of 0.27 km s^{-1}, and (2) the velocity resolution of 0.22 km s^{-1}, is far smaller than the radial velocity dispersion of 4.81 km s^{-1}. Thus, the correction for the broadening effect in radial velocity dispersion is not very important and so is not taken into account in our calculations. All the parameters used to calculate the distance are summarized in Table 3.

From Equation (1) we obtain the distance to VX Sgr to be 1.40 and 1.63 kpc using the proper motions in R.A. and Dec. between epoch 1 and epoch 2, and to be 1.55 and 1.87 kpc using the proper motions in R.A. and Dec. between epoch 1 and epoch 3.

The fractional uncertainty in the distance derived from Equations (1) and (2) is given by

$$\frac{\sigma_D}{D}=\Big\{\frac{1}{2M}+\frac{1}{2N}\Big[1-\left(\frac{\epsilon_{\rm obs}}{\sigma_\mu^{\rm obs}}\right)^2\Big]^{-1}\Big\}^{1/2}, \tag{3}$$

where M is the number of features used for estimating the radial velocity dispersion, N is the number of maser features with measured relative proper motions. In our calculations, M=325, N=42. The obtained distance and its uncertainty are also listed in Table 3.

From Table 3, we can see that the obtained distances are different in R.A. and Dec. from both epoch 2–1 and epoch 3–1. This may reflect asymmetric distributions of proper motion dispersions in R.A. and Dec. Table 3 also shows that the distances in R.A. and Dec. are distinctly larger for epoch 3–1 than for epoch 2–1, suggesting systematic errors when aligning the maps of the three epochs or time variation of proper motion between epoch 2–1 and epoch 3–1. So, to get a more reasonable estimate of the distance, we first compute the weighted mean of distances in R.A. and Dec. (with weights computed from inverse squares of the errors in distance) for epoch 2–1 and epoch 3–1. The distance obtained for epoch 2–1 is 1.48$\pm$0.14 kpc and that for epoch 3–1 is 1.65$\pm$0.16 kpc, so we obtain a final value of 1.57$\pm$0.19 kpc.

However, there are several other sources of systematic errors. Systematic effects, such as a bias in the estimate of the measurement error, uncertainty in the rest velocity of the system, asymmetries in the transverse and radial velocity distributions, the asymmetrical distribution of the maser features, and the global expansion or contraction of maser shell, all contribute to the uncertainty in the distance. It is difficult to estimate the uncertainty due to these systematic effects. As a conservative estimation based on the mean of Schenps et al. (1981), the uncertainty in distance after taking systematic effects into account is $\pm$0.27 kpc, which is about $\sqrt{2}$ times the above value of $\pm$0.19 kpc.

The estimated distance of 1.57$\pm$0.27 kpc to VX Sgr is in agreement with that based on proper motions of H_2O masers (1.7–1.8 kpc, Marvel et al. 1998; Murakawa et al. 2003), or on the assumption that VX Sgr is associated with the Sgr OB1 association (1.7–2.0 kpc, see Table 1), at which distance VX Sgr is indeed a red supergiant.

4 DISCUSSION

This is the first time that an astronomical distance is measured using SiO masers. SiO masers are now known to be associated with a very wide range of circumstellar objects, from short-period, low-mass-loss Mira variables to extremely long-period, high-mass-loss OH/IR stars, from supergiant variables to symbiotic variables. SiO masers are good astrometry candidates because they themselves are very bright as well as

Table 4 Previous Results of Distance Measurements Using Masers

Source	Maser	Method[a]	Distance	Reference
Interstellar masers				
Orion KL	H_2O	MF	480±80 pc	Genzel et al. (1981a)
W51 Main	H_2O	SP	7±1.5 kpc	Genzel et al. (1981b)
W51 North	H_2O	SP	8.3±2.5 kpc	Schneps et al. (1981)
Sgr B2 North	H_2O	MF	7.1±1.5 kpc	Reid et al. (1988a)
Sgr B2 Middle	H_2O	MF	6.5±1.5 kpc	Reid et al. (1988b)
W49 North	H_2O	MF	11.4±1.2 kpc	Gwinn et al. (1992)
Cep A	H_2O	SP	500±200 pc	Cawthorne et al. (1993)
W3 IRS5	H_2O	MF	1.81±0.10 kpc	Imai et al. (2000)
W3(OH)	H_2O	AP	2.04±0.07 kpc	Hachisuka et al. (2006)
W3(OH)	CH_3OH	AP	1.95±0.03 kpc	Xu et al. (2006)
Circumstellar masers				
S Persei	H_2O	MF	2.3±0.5 kpc	Marvel (1998)
VY Canis Majoris	H_2O	MF	1.4±0.2 kpc	Marvel (1998)
VX Sgr	H_2O	MF	1.7±0.3 kpc	Marvel (1998)
VX Sgr	H_2O	MF	1.8±0.5 kpc	Murakawa et al. (2003)
U Herculis	OH	AP	189^{+123}_{-54} pc	Langevelde et al. (2000)
U Herculis	OH	AP	277^{+112}_{-62} pc	Vlemmings et al. (2003)
W Hya	OH	AP	98^{+30}_{-18} pc	Vlemmings et al. (2003)
S CrB	OH	AP	433^{+72}_{-54} pc	Vlemmings et al. (2003)
R Cas	OH	AP	176^{+92}_{-45} pc	Vlemmings et al. (2003)
UX Cyg	H_2O	AP	$1.85^{+0.25}_{-0.19}$ kpc	Kurayama et al. (2005)

[a]MF: Model fitttig; SP: statistical parallax; AP: annual parallax

being abundantly located in a ring close to the star (typical 2–4 R_* for late-type stars, Diamond et al. 1994). An important aspect of SiO maser astrometry is the tie between the IR and radio positions in the Galactic center. By locking the positions of the IR sources to the radio maser counterparts, it can be shown that the motion of stars in the Galactic center is consistent with motion around a massive black hole located at the position of Sgr A^* (Menten et al. 1997; Schödel et al. 2002). Unfortunately, so far few SiO masers are directly made use of measuring distance.

Depending on the obtained kinematics for masers, there are two methods used to obtain the proper motion distance. One is the statistical parallax method as discussed in this paper. Another is to compare three-dimensional kinematic models with the observed kinematics for masers, and the source distance can be obtained as one of the free parameters of the best kinematic model. This method may be called "model fitting method", which could be applied only when the kinematics for masers are dominated by some systematic motion, such as due to an expansion, a contraction or a rotation (see details in Imai et al. 2000). Moreover, at the moment, the most powerful tool for the determination of distances to objects in our Galaxy is direct measurement of annual parallaxes of the maser sources, because the distances can be measured without any assumptions in this measurements. We summarize some previous results of distance measurements using masers in Table 4.

From Table 4 one can see that more accurate distances have been successfully obtained by measuring the annual parallaxes of OH, H_2O and CH_3OH masers. However, the measurement of an annual parallax is very difficult for SiO masers due to limitations in the present VLBI technology. The coherence time is only on the order of a few tens of seconds and there are very few available extragalactic calibrators at 43 GHz. In addition, often SiO masers are short-lived (lifetimes of weeks) and their motions are not linear. The "model fitting" method using SiO maser sources is also difficult because the kinematics within SiO maser regions are complex, being dominated by mass-loss and permeated by shocks, magnetic fields and density gradients. An SiO maser movie of Mira variable TX Cam has displayed the co-existence of both local infall and outflow motions at a certain stellar phase (Diamond & Kemball 2003). Our observations also show that the motions of individual maser features around VX Sgr are relatively random, making it very difficult to measure distance by the model fitting method. Thus, the statistical parallax method may be among the best to measure the distances of SiO masers.

5 CONCLUSIONS

In the circumstellar envelope of the M-type semi-regular variable star VX Sgr, v=1, J=1–0 SiO maser proper motions at 43 GHz were obtained by our 3-epoch VLBA monitoring observations over 39 days in 1999 April–May. We apply the statistical parallax analysis on these proper motions to measure the distance of VX Sgr. The estimated distance of VX Sgr of 1.57 ± 0.27 kpc is consistent with that based on the proper motions of H_2O masers, or on the assumption that VX Sgr belongs to the Sgr OB1 association, at which VX Sgr is indeed a red supergiant.

Acknowledgements This work was supported in part by the National Natural Science Foundation of China (Grant 10573029) and sponsored by Program of Shanghai Subject Chief Scientist (06XD14024). Z.-Q. Shen acknowledges the support by the One-Hundred-Talent Program of Chinese Academy of Sciences.

References

Alter G., Balázs B., Ruprecht J., eds., 1970, Catalogue of Star Clusters and Associations (2d ed., Budapest: Akad. Kiadó), 2379
Cawthorne T. V., Moran J. M., Reid M. J., 1993, In A. W. Clegg, G. E. Nedoluha, eds., Astrophysical Masers, Heidelberg, FRG, p.65
Celis L., 1975, A&AS, 22, 9
Chapman J. M., Cohen R. J., 1986, MNRAS, 220, 513
Chen X., Shen Z. Q., Imai H., Kamohara R., 2006, ApJ, 640, 982 (Paper I)
Diamond P. J., Kemball A. J., 2003, ApJ, 599, 1372
Diamond P. J., Kemball A. J., Junor W. et al., 1994, ApJ, 430, L61
Genzel R., Downes D., Schneps M. H. et al., 1981a, ApJ, 247, 1039
Genzel R., Reid M. J., Moran J. M., Downes D., 1981b, ApJ, 244, 884
Greenhill L. J., Colomer F., Moran J. M. et al., 1995, ApJ, 449, 365
Gwinn C. R., Moran J. M., Reid M. J., 1992, ApJ, 393, 149
Hachisuka K., Brunthaler A., Menten K. et al., 2006, ApJ, 645, 337
Humphreys R. W., Spencer J. H., Bowers P. E., 1972, ApJ, 172, 75
Humphreys R. W., 1974, ApJ, 188, 75
Imai H., Miyoshi M., Deguchi S. et al., 2000, ApJ, 538, 751
Kamohara R., Deguchi S., Miyoshi M., Shen Z.-Q., 2005, PASJ, 57, 341
Kukarkin B. V., Khopopov P. N., Efremov Y. N. et al., 1970. Catalogue of Variable Stars, Astronomical Council of the Academy of Sciences in the USSR, Moscow.
Kurayama T., Sasao T., Kobayashi H., 2005, ApJ, 627, L49
Langevelde H. J., van Vlemmings W., Diamond P. J. et al., 2000, A&A, 357, 945
Lockwood G.W., Wing R. F., 1982, MNRAS, 198, 385
Loup C., Forveille T., Omont A., Paul J. F., 1993, A&AS, 99, 291
Marvel K. B., Diamond P.J., Kemball A. J., 1998, In: J. A. Zensus, G. B. Taylor, J. M., Wrobel, eds., ASP Conf. Ser. Vol. 144, p.253
Menten K. M., Reid M. J., Eckart A., Genzel R., 1997, ApJ, 475, L111
Morgan W. W., Whitford A. E., Code A. D., 1953, ApJ,118, 318
Murakawa K., Yates J. A., Richards A. M. S., Cohen R. J., 2003, MNRAS, 344, 1
Pourbaix D., Platais I., Detournay S. et al., 2003, A&A, 399, 1167
Reid M. J., Gwinn C. R., Moran J. M., Matthews A. H., 1988a, BASS, 20, 1017R
Reid M. J., Schneps M. H., Moran J. M. et al., 1988b, ApJ, 330, 809
Schneps M. H., Lane A. P., Downes D. et al., 1981, ApJ, 249, 124
Schödel R., Ott T., Genzel R. et al., 2002, Nature, 419, 694
Vlemmings W. H. T., Van Langevelda H. J., Diamond P. J. et al., 2003, A&A, 407, 213
Xu Y., Reid M. J., Zheng X. W., Menten K. M., 2006, Science, 311, 54